

Effect of Preprocessing and Augmentation Process in Development of a Deep Learning Model for Fusarium Detection in Shallots

Yuvicko Gerhaen Purwansya¹, Mohamad Solahudin^{1,✉}, Supriyanto¹

¹ Department of Mechanical and Biosystem Engineering, Faculty of Agricultural Engineering and Technology, IPB University, Bogor, INDONESIA.

Article History:

Received : 06 June 2023
Revised : 19 October 2023
Accepted : 29 December 2023

Keywords:

Augmentation,
Deep learning,
Fusarium,
Shallot.

Corresponding Author:

✉ mohamadso@apps.ipb.ac.id
(Mohamad Solahudin)

ABSTRACT

As the demand for shallot increases, wide-scale cultivation area must be managed efficiently. However, shallot productivity decreases every year because of plant diseases. Fusarium disease has an intensity up to 60% and can affect yield losses up to 50%. This study was conducted to develop the fusarium disease detection system for shallot using deep learning model and analyze the effect of preprocessing and augmentation adjustment. This study used YOLOv5 deep learning algorithm consisting of the following stages: (1) dataset acquisition, (2) dataset annotation, (3) dataset preprocessing and augmentation, (4) dataset training and validation, and (5) model testing and evaluation. A total 9,664 annotated dataset was trained to YOLOv5m pre-trained weights. Based on testing and evaluation results, precision, recall, and mean average precision (mAP) metrics of the model without preprocessing and augmentation were 55.5%; 54%; and 48.3% respectively. Metric values of the model were increased to 57.6%; 58.4%; and 54.1% respectively with adjustment of preprocessing and augmentation combination process. Percentage increase in metrics when compared to the control model for each value of precision, recall, and mAP were 2.1%; 4.4%; and 5.8%. This shows a significant impact on the addition of preprocessing and augmentation processes that match the characteristics of the dataset to increase the value of model performance.

1. INTRODUCTION

Shallot is one of the main functional food commodities for human. World shallot cultivation has increased 101.4% from 2.46 million hectares in 1996 to 4.95 million hectares in 2016. Besides that, total production in 2016 has increased 128,94% from 40.69 million tons to 93.17 million tons (Hanci, 2018). With the increases of shallot demand, wide-scale cultivation area must be managed efficiently. However, shallot cultivation until this day has decreased because of diseases and affect to more than 50% yield loss in the fields (Harvey *et al.*, 2014). Fusarium disease, usually called moler disease, is one of the problems in shallot cultivation caused by *Fusarium oxysporum* sp. Disease intensity can be up to 60% in shallot cultivation and has been reported to be an important threat that can affect yield losses up to 50% (Supyani *et al.*, 2021). Despite from that, monitoring growth and disease of shallots is important to prevent plant damage that affected by pests and diseases and minimize yield loss (Lu *et al.*, 2017; Solahudin *et al.*, 2015).

Unmanned aerial vehicle (UAV) integrated with artificial intelligence is one of developed technology that can be used for visual monitoring plant condition in shallot cultivation (Singh *et al.*, 2021; Solahudin & Mutawally, 2020). Machine vision is one of artificial intelligence algorithm that can be used for detect physical characteristic of plants based on

machine vision parameter of red-green-blue (RGB). Nowadays, machine vision application is widely developed with integration of UAV (Atefi *et al.*, 2021) so that can faster the high-resolution image acquisition with support the global positioning system (GPS) feature in large area of plant cultivation (Feng *et al.*, 2021). Deep learning is advanced part of machine learning algorithm using artificial neural networks which have the potential to be used for detecting plant disease symptoms (Ahmad *et al.*, 2023; Ferentinos, 2018). An example of deep learning application research is the detection of symptoms of shallot downy mildew disease automatically based on deep neural networks (Kim *et al.*, 2020).

The objectives of this research are to develop a deep learning model for a shallot fusarium wilt disease detection system using the image of an UAV and analyze its effect on the addition of preprocessing and augmentation process. This research is a development from previous UAV and RGB camera application with artificial neural network researches for visual monitoring shallot diseases. Deep learning is used in this research to develop plant diseases monitoring system that detect specific to fusarium diseases. YOLOv5 algorithm is used for specific real time object detection model with the advantages of fast, precise, and easy to train. This disease detection system was developed to be able to solve disease monitoring problems quickly and accurately compared to using either technology alone or conventional methods (Neupane & Baysal-Gurel, 2021).

2. METHODOLOGY

Research was conducted from January to May 2023. Dataset acquisition of shallot plants was taken and located at one of farmer's shallot fields at Wanasari Village, Wanasari District, Brebes Regency, Central Java (-6.895233° S, 109.018127° E). Details for the acquisition area is described with polygon in Figure 1. Dataset processing and model development were carried out at Bioinformatics Engineering Laboratory, Department of Mechanical and Biosystem Engineering, IPB University.

Tools in this research were separated into hardware and software. Hardwares included DJI Mavic Air Drones that include RGB camera and one set laptop Acer Aspire 5 A514-54G 11thGen Intel® Core™ i7-1165G7 NVIDIA GeForce MX350 that include Python programming language. YOLOv5 algorithm was used for data analysis and model development. Softwares that used are DJI GO 4 for data acquisition from drone, then Roboflow and Google Colaboratory for data analysis and model development. Workflow diagram of research methodology was shown in the flowchart in Figure 2.

2.1. Dataset Acquisition

Dataset acquisition was done for the main objects to develop shallot disease detection deep learning model. Firstly, location survey must be done to identify shallot fields that have fusarium symptoms. Once identified, then the characteristics of the fields were recorded and can be started to collect shallot image data using UAV and direct recording of each point of the plant in the fields. According to land suitability research by Susilawati *et al.*, (2019) (Figure 1), Wanasari Village, Wanasari District, Brebes Regency is good for shallot cultivation with land suitability at the S2 level (quite suitable) and dominant S3 (marginally appropriate).

2.2. Dataset Annotation

Object labeling or annotation was done after the dataset has been collected and identified. Object labeling is done to find out which objects will be recognized in an image. Labeling was needed so that the object can be recognized during the deep learning training process. The object labeling stage was by marking the bounding box on the dataset identified for the training data process which was carried out at a later stage. The result of this process is in the form of an annotation of the labeling results in the form of a text file that has information of bounding boxes coordinate and size.

2.3. Dataset Preprocessing and Augmentation

Usually, there are still disturbances or biases in images directly captured by the camera that reduce the performance of the training dataset, such as the effects of focus, vibration, differences in color and lighting, as well as interference from objects other than the main object (Ali *et al.*, 2019). This was anticipated by carrying out preprocessing and augmentation processes on the annotated dataset to avoid the influence of the bias that previously mentioned.

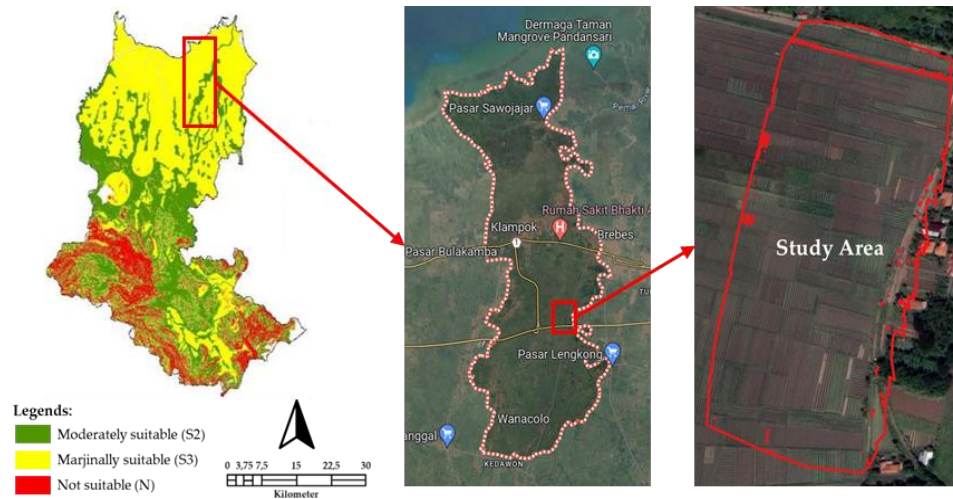


Figure 1. Location of the study area

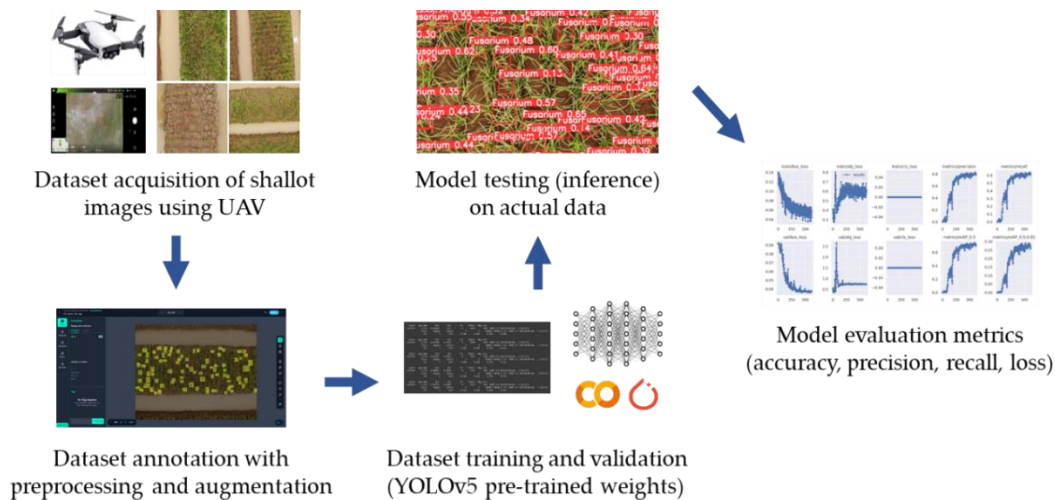


Figure 2. Research workflow of shallot fusarium disease detection deep learning model development

Preprocessing process is applied to the training, validation, and testing datasets. The advantage of preprocessing process is that it can speed up training time and improve model performance (Chen *et al.*, 2022). Preprocessing can be done by resizing the image, rotating the image, cutting the image into several parts, and changing color features such as adjusting the image contrast. The augmentation process is applied to the training data to create a variation of examples in the training dataset so as to improve model generalization performance (Dang *et al.*, 2023). The augmentation process is based on setting the orientation and color of the image or bounding boxes which can be adjusted according to the needs and characteristics of the dataset being developed (Liu *et al.*, 2023).

Research from Zhang *et al.*, (2022) use geometric distortion correction and the grayscale stretch preprocessing algorithm for increasing image contrast in automatic stomata recognition and measurement, while research from Dang *et al.*, (2023) use one of the ten geometric and photometric transformations randomly to improve model performance in object detection with augmentation features in research on weed detection in cotton plants based on the YOLO deep learning model.

2.4. Dataset Training and Model Evaluation

Dataset training is the process of setup an algorithm model created to train the dataset that has been collected. This process uses annotation files collected from the dataset annotation results. Dataset training for fusarium shallot disease detection based on visual symptom was implemented in Google Colaboratory notebook with Graphic Processing Unit (GPU) were used Python 3 Google Compute Engine backend (GPU).

YOLO algorithm work principle in object detection based on 24 layers of convolutional neural networks (CNN) which consist connected, activation, and pooling layers for the process. YOLO divides the input image into an $S \times S$ grid and each grid cell predicts a number of bounding boxes and their confidence value (Redmon *et al.*, 2016). Confidence value represent how accurate the model detects the object. If no object exists in that cell, the confidence value is 0. Confidence value must be greater or equal than intersection over union (IOU) between the predicted box and the actual object. YOLO algorithm concept in object detection is illustrated in Figure 3.

This research used 5th version of YOLO algorithm (YOLOv5) by Ultralytics that have better performance than older version. YOLOv5 has five pre-trained models whose characteristics vary in aspect of weight size and average learning speed. Available version of YOLOv5 pre-trained model is nano, small, medium, large, and extra large. All five of them can provide options for users to adjust to the hardware that will be used so that it can run properly.

To evaluate the performance of the model, metrics performance table of was used. The mean average precision (mAP) was used as the metric value for performance evaluation of the fusarium shallot disease detection symptom model (Kim *et al.*, 2020). It was the mean value of each class's average precision (AP) that calculated by recall (r) and precision (p) metrics (Shen *et al.*, 2018). Precision is the probability value of the actual positive object of all the objects that are predicted to be positive. The precision value can measure the accuracy of the prediction of positive sample results, while recall is the probability value of the actual positive object from all possible predicted object so that the recall value can represent the overall prediction accuracy (Liu *et al.*, 2023). Equation of mAP, precision, and recall are represented as the following:

$$\text{mAP} = \frac{1}{n} \sum_{k=1}^n AP_k \quad (1)$$

$$\text{Precision} = \frac{TP}{TP+FP} \quad (2)$$

$$\text{Recall} = \frac{TP}{TP+FN} \quad (3)$$

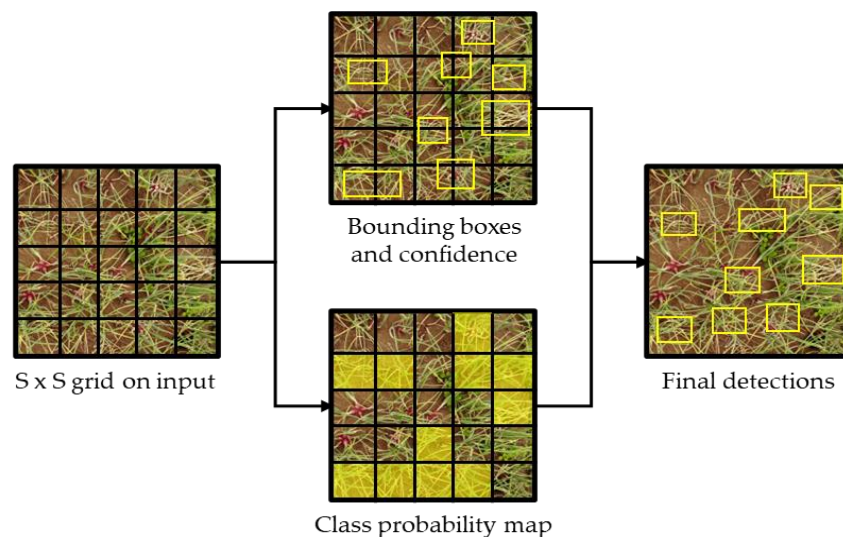


Figure 3. YOLO algorithm concept in object detection

In the mAP equation, the n value shows the number of classes detected while the AP_k shows the average precision (AP) value for each class k . True positive (TP) means that the prediction result and the basic sample truth value are positive, while true negative (TN) means that the prediction result and the basic sample truth value are negative. False positive (FP) indicates that the prediction result is positive and the basic truth value is negative. False negative (FN) indicates that the prediction result is negative and the basic truth value is positive (Chen *et al.*, 2022).

3. RESULTS AND DISCUSSION

3.1. Dataset Acquisition Result

Detailed information from the results of the data acquisition process is described in Figure 4. The dataset is collected in the form of images taken by the UAV Drone DJI Mavic Air with an RGB camera with a height of 5 meters and an image resolution of 4056×3040 pixels. Acquisition time between 11:30 and 13:30 Western Indonesia Time is very good for avoiding shadows formed by sunlight (Kerkech *et al.*, 2020). The images taken are shallots (*Allium cepa* L.) aged 10 - 50 days, namely after the growth of shoots and before the ripening period. The spacing of shallots planted on the land is 15×15 cm. Currently shallot plants are very susceptible to disease due to high air humidity. Under high humidity conditions, the *Fusarium oxysporum* fungus can easily grow on shallots which can cause fusarium wilt.

The collected images of 130 images are used for YOLOv5 model development data and a total of 9,664 annotations were produced which were divided into 3 classes (fusarium, shallot, and weeds) as training and validation data. Fusarium class indicates shallot plants with symptoms of fusarium disease, marked by yellowing and wilting of the tips of the stems to the leaves (Yang *et al.*, 2022). The specific difference between shallots that are attacked by fusarium wilt and other diseases is that the point of attack is at the base of the tuber. *Fusarium oxysporum* can be seen at the base of the bulb which is whitish in color, whereas if the tuber is cut lengthwise, it will show the part that is rotting. Shallot class shows shallot plant objects that are still 10 - 15 days old, and weeds class shows weeds growing around shallot fields. Ratio of images for training and validation is 80% : 20% (104 : 26 images). There are 84 images (65%) of the 130 images that show symptoms of fusarium attacks. Each image was taken from a total of 48 shallot plots at the research location so that maximum 3 images were taken from each plot. Total area of the research land is 5.2 hectares so the average area of shallot plots is 0.11 hectares. The distribution of annotations on the dataset for each class is shown in Table 1 and details of the data classification are shown in Figure 5. Figure 6 shows an example of a dataset taken by visualizing each class made.

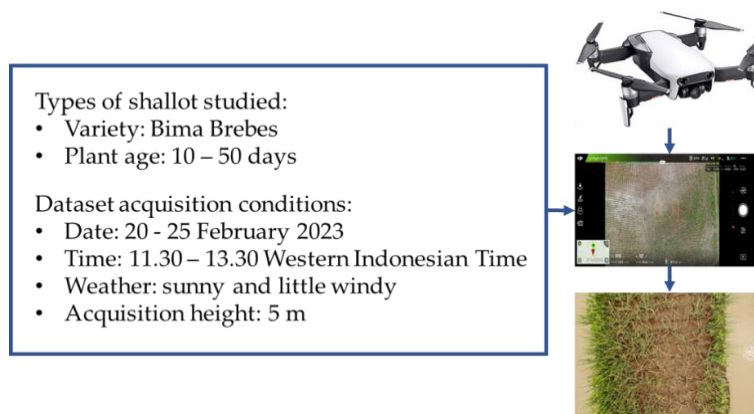


Figure 4. Information of data acquisition process

Table 1. Annotation distribution of dataset

Class	Training set (80%)	Validation set (20%)	Total
Fusarium	2,017	554	2,571
Shallot	3,047	497	3,544
Weeds	2,435	1,114	3,549
Total	7,499	2,165	9,664

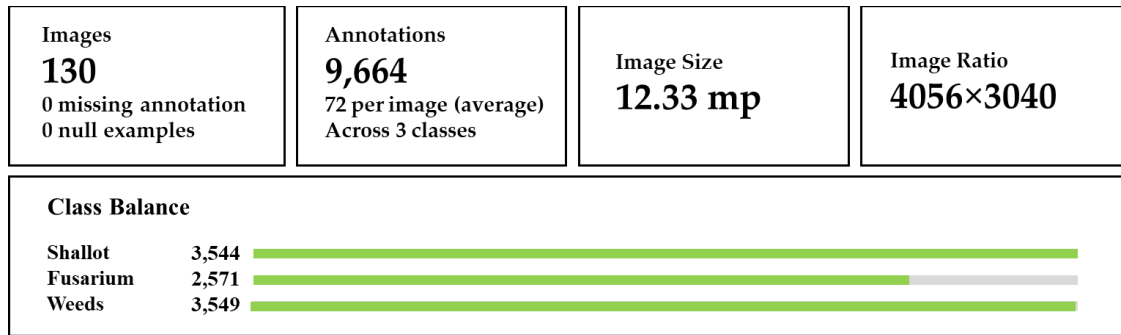


Figure 5. Result of data classification



Figure 6. Example of dataset images. (a) Shallots. (b) Fusarium. (c) Weeds

3.2. Model Development Result

The details of the model used for the training process are described in Table 2. The dataset was trained using 500 epochs with a patience value of 100 so that when the training process shows convergent results for 100 running epochs, the training process will stop earlier before the predetermined epochs value.

Figure 7 and 8 shows the loss curves in each category for a total of 231 epochs. Each graph shows a change in the loss value that decreases each running epoch for the training data and gradually becomes constant close to zero. The loss curve for box validation and class validation shows a drastic decrease and is closer to zero, but for object validation at the initial epoch it moves constant then the curve increases gradually with fluctuations. This shows the occurrence of overfitting in the model. The training process will stop based on hyper-parameter setup and generalization performance. This can minimize the occurrence of overfitting in the training process because the model is considered convergent (Kim *et al.*, 2020). In this condition, the best model weight is in the 130th epochs because after 231 epochs running there is no performance increase in the model.

Table 2. Model training parameter

Training hyper-parameter	Description
Sub model	YOLOv5m
Total layers	291 layers
Optimizer	Stochastic Gradient Descent (learning rate = 0,01)
Image size (training)	640 × 640 px
Batch	16
Epoch	500
Patience	100
Save period	100

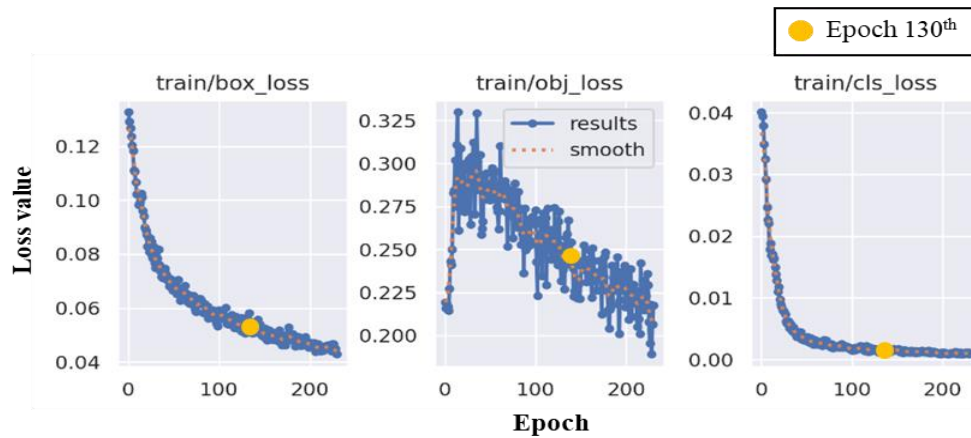


Figure 7. Train loss graphics of model training result



Figure 8. Validation loss graphics of model training result

Table 3. Result of model training process

Class	Validation Images	Instances	Precision	Recall	mAP@0.5	mAP@[0.5:0.95]
All	26	2,165	0.555	0.54	0.483	0.19
Fusarium		554	0.467	0.298	0.289	0.0915
Shallot		497	0.629	0.702	0.591	0.211
Weeds		1,114	0.569	0.62	0.57	0.268

The results of the training process are shown in Table 3. The highest metric values are in the shallot class while the lowest is fusarium. The highest mAP@0.5 value was owned by the shallot class, but the highest mAP@[0.5:0.95] was owned by the weed class. This indicates that the weed class has a better average level of precision due to prediction results with an intersects over union (IoU) of 50% – 95% more weed classes than other classes. The precision value of all classes (55.5%) shows that of all the predictions made by the model that classified three object classes as positive, around 55.5% of the predictions were true. The recall value of all classes (54%) shows that of all cases of object detection in the datasets, the model was able to identify around 54% of these cases correctly. The results show that the value of the model development metric is still not good enough. This is caused by the fusarium class which has the complexity of image features in its dataset, which can reduce the performance of the training process (Ali *et al.*, 2019). The fusarium class has a focus on detection features on specific parts of the shallot plant that are attacked by the fungus *Fusarium oxysporum*, starting from the tips of the leaves that turn yellow and twisted then wither until they reach the stem of the plant (Yang *et al.*, 2022), and YOLO algorithm detect this symptom in their architecture with the result of inference

shown in Figure 9. Besides that, the condition of complex and abstract plant objects also affects the low mAP value of the fusarium class. The detected shallot plant objects are around 40 - 50 days old so the shallot plants have grown large and with close spacing causes the plants to overlap one another (Hanci, 2018). This can be a challenge during the annotation process because it is necessary to prepare accurate image features for the convolution layer in the YOLO model so that objects can be identified more specifically than other objects (Bochkovskiy *et al.*, 2020; Redmon *et al.*, 2016; Wang *et al.*, 2022). The addition of preprocessing and augmentation processes has the potential to overcome the problem of object complexity in this study so that model performance can be increased. Moreover, the performance of the model in detecting the object being trained will be better if more datasets with vary conditions are used. This is because the model created will be trained better with many object variations conditions that have been classified (Li *et al.*, 2022). An example of the results of model detection is shown in Figure 9.

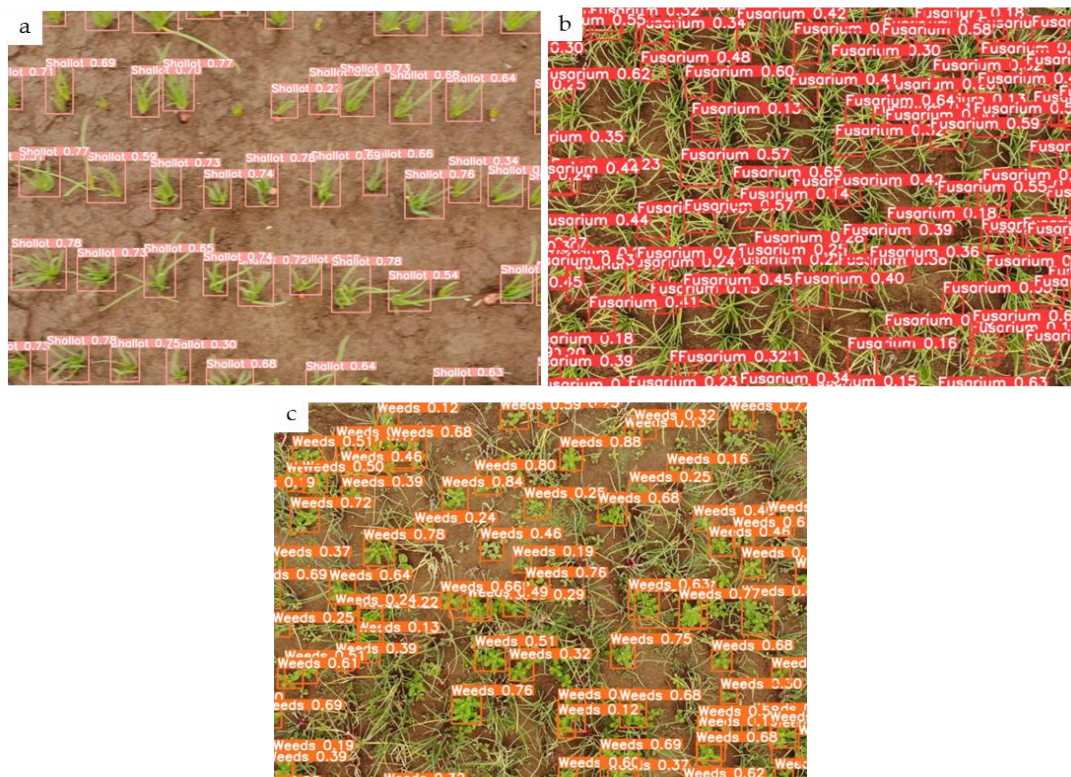


Figure 9. Example of model class inference result. (a) Shallots. (b) Fusarium. (c) Weeds

Table 4. Result of model combination training comparison

Models	Best Epochs	Time (hours)	Precision	Recall	mAP@0.5	mAP@[0.5:0.95]
YOLOv5	130	0.46	0.555	0.54	0.483	0.19
YOLOv5 with preprocessing	64	0.35	0.544	0.547	0.515	0.18
YOLOv5 with augmentation	32	0.68	0.569	0.567	0.529	0.19
YOLOv5 with preprocessing and augmentation	48	0.86	0.576	0.584	0.541	0.2

3.3. Adjustment of Preprocessing and Augmentation Process

This section compares the control model that has been developed in the previous section, with its effect on the addition of preprocessing and augmentation. The process combinations in the model are shown in Table 4 and compared by total epochs and model performance metric values. Preprocessing process on the model dataset uses the histogram

equalization adjustment contrast feature. For augmentation, the features rotate (90° and 180°), crop (maximum 50%), saturation variety (between -25% and 25%), and noise adjustment (maximum 5%) are used. All of these features were chosen because they are suitable for research datasets that are aerial imagery by drones and require color parameters to detect objects (Bao *et al.*, 2023). The process illustration for each additional feature is depicted in Figures 10 and 11.

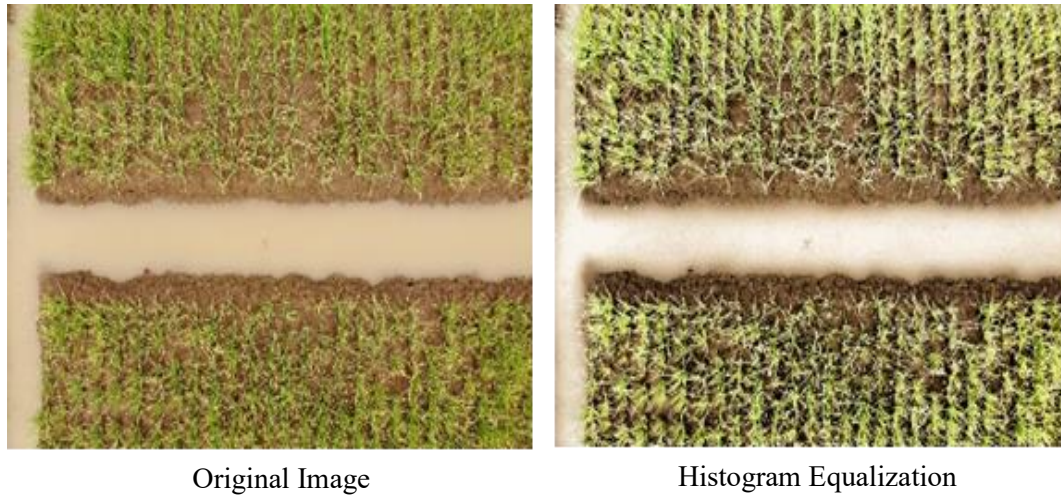


Figure 10. Illustration of preprocessing process

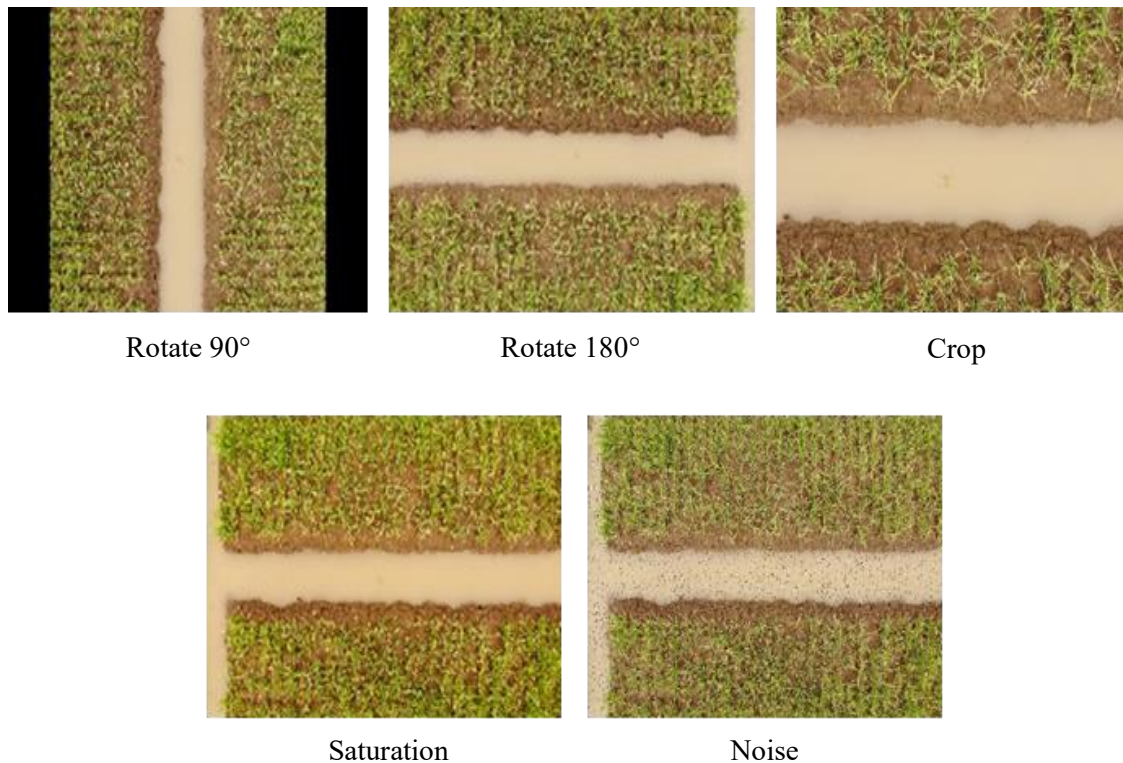


Figure 11. Illustration of augmentation process

Based on the results of the combination training model in Table 4, there is an increase in the performance value of the model if the preprocessing and augmentation features are added. The combination model with the best improvement is

the model with additional preprocessing and augmentation processes. The percentage increase in performance metrics when compared to the control model for each precision, recall, mAP@0.5, and mAP@[0.5:0.95] value is 2.1%; 4.4%; 5.8%; and 1.0%. The results of this increase show a significant impact on the addition of preprocessing and augmentation processes that match the characteristics of the dataset to increase the value of model performance (Luo *et al.*, 2023). However, in the length of time of the training process, the model with the addition of preprocessing and augmentation has the longest time compared to the other combinations, and that is even 2 times longer than the control model. This is because the model needs to process more datasets due to the addition of dataset variations from the augmentation feature (Chen *et al.*, 2022). If combined with the preprocessing process, the dataset variations will increase. For this reason, the addition of these two features has its own advantages and disadvantages relative to the characteristics of the dataset being developed (Sanaeifar *et al.*, 2023). Need to choose the right combination of preprocessing and augmentation processes in order to improve model performance and not add too much time to the training process.

4. CONCLUSIONS

Development of deep learning model to monitor the growth of shallot can be implemented to prevent plant damage due to diseases and minimize yield losses. This research provides shallot fusarium diseases dataset taken by the UAV Drone DJI Mavic Air with an RGB camera and collected 145 images. A total of 130 images were selected and a total of 9,664 annotations were produced which were divided into 3 classes (fusarium, shallot, and weeds) as training and validation data. Results of precision, recall, mAP@0.5, and mAP@[0.5:0.95] value of the model were 55.5%; 54%; 48.3%; and 19.0% respectively. With the adjustment of preprocessing and augmentation process, metric values of the model were increased to 57.6%; 58.4%; 54.1%; and 20.0% respectively. Percentage increase in metrics when compared to the control model for each value of precision, recall, mAP@0.5, and mAP@[0.5:0.95] is 2.1%; 4.4%; 5.8%; and 1.0%. The results of this increase show a significant impact on the addition of preprocessing and augmentation processes that match the characteristics of the dataset to increase the value of model performance.

REFERENCES

- Ahmad, A., Saraswat, D., & El Gamal, A. (2023). A survey on using deep learning techniques for plant disease diagnosis and recommendations for development of appropriate tools. *Smart Agricultural Technology*, **3**, 100083. <https://doi.org/10.1016/j.atech.2022.100083>
- Ali, M.M., Bachik, N.A., Muhadi, N., Yusof, T.N.T., & Gomes, C. (2019). Non-destructive techniques of detecting plant diseases: A review. *Physiological and Molecular Plant Pathology*, **108**, 101426. <https://doi.org/10.1016/j.pmpp.2019.101426>
- Atefi, A., Ge, Y., Pitla, S., & Schnable, J. (2021). Robotic technologies for high-throughput plant phenotyping: Contemporary reviews and future perspectives. *Frontiers in Plant Science*, **12**, <https://doi.org/10.3389/fpls.2021.611940>
- Bao, W., Zhu, Z., Hu, G., Zhou, X., Zhang, D., & Yang, X. (2023). UAV remote sensing detection of tea leaf blight based on DDMA-YOLO. *Computers and Electronics in Agriculture*, **205**, 107637. <https://doi.org/10.1016/j.compag.2023.107637>
- Bochkovskiy, A., Wang, C.Y., & Liao, H.Y.M. (2020). YOLOv4: Optimal speed and accuracy of object detection. *arXiv*, **2004**, 10934v1. <https://doi.org/10.48550/arXiv.2004.10934>
- Chen, J., Wang, H., Zhang, H., Luo, T., Wei, D., Long, T., & Wang, Z. (2022). Weed detection in sesame fields using a YOLO model with an enhanced attention mechanism and feature fusion. *Computers and Electronics in Agriculture*, **202**, 107412. <https://doi.org/10.1016/j.compag.2022.107412>
- Dang, F., Chen, D., Lu, Y., & Li, Z. (2023). YOLOWeeds: A novel benchmark of YOLO object detectors for multi-class weed detection in cotton production systems. *Computers and Electronics in Agriculture*, **205**, 107655. <https://doi.org/10.1016/j.compag.2023.107655>
- Feng, L., Chen, S., Zhang, C., Zhang, Y., & He, Y. (2021). A comprehensive review on recent applications of unmanned aerial vehicle remote sensing with various sensors for high-throughput plant phenotyping. *Computers and Electronics in Agriculture*, **182**. <https://doi.org/10.1016/j.compag.2021.106033>
- Ferentinos, K.P. (2018). Deep learning models for plant disease detection and diagnosis. *Computers and Electronics in Agriculture*, **145**, 311–318. <https://doi.org/10.1016/j.compag.2018.01.009>
- Hanci, F. (2018). A Comprehensive overview of onion production: Worldwide and Turkey. *Journal of Agriculture and Veterinary Science*, **11**(9), 17–27. <https://doi.org/10.9790/2380-1109011727>

- Harvey, C.A., Rakotobe, Z.L., Rao, N.S., Dave, R., Razafimahatratra, H., Rabarijohn, R.H., Rajaofara, H., & MacKinnon, J.L. (2014). Extreme vulnerability of smallholder farmers to agricultural risks and climate change in Madagascar. *Philosophical Transactions of the Royal Society B: Biological Sciences*, **369**(1639). <https://doi.org/10.1098/rstb.2013.0089>
- Kim, W.S., Lee, D.H., & Kim, Y.J. (2020). Machine vision-based automatic disease symptom detection of onion downy mildew. *Computers and Electronics in Agriculture*, **168**, 105099. <https://doi.org/10.1016/j.compag.2019.105099>
- Li, R., Wang, R., Xie, C., Chen, H., Long, Q., Liu, L., Zhang, J., Chen, T., Hu, H., Jiao, L., Du, J., & Liu, H. (2022). A multi-branch convolutional neural network with density map for aphid counting. *Biosystems Engineering*, **213**, 148–161. <https://doi.org/10.1016/j.biosystemseng.2021.11.020>
- Liu, Q., Zhang, Y., & Yang, G. (2023). Small unopened cotton boll counting by detection with MRF-YOLO in the wild. *Computers and Electronics in Agriculture*, **204**, 107576. <https://doi.org/10.1016/j.compag.2022.107576>
- Lu, J., Hu, J., Zhao, G., Mei, F., & Zhang, C. (2017). An in-field automatic wheat disease diagnosis system. *Computers and Electronics in Agriculture*, **142**(1), 369–379. <https://doi.org/10.1016/j.compag.2017.09.012>
- Luo, K., Jin, Y., Wen, S., Li, Y., Rong, J., & Ding, M. (2023). Detection and quantification of cotton trichomes by deep learning algorithm. *Computers and Electronics in Agriculture*, **210**, 107936. <https://doi.org/10.1016/j.compag.2023.107936>
- Neupane, K., & Baysal-Gurel, F. (2021). Automatic identification and monitoring of plant diseases using unmanned aerial vehicles: A review. *Remote Sensing*, **13**(19). <https://doi.org/10.3390/rs13193841>
- Redmon, J., Divvala, S., Girshick, R., & Farhadi, A. (2016). You only look once: Unified, real-time object detection. *Proceedings of the IEEE Computer Society Conference on Computer Vision and Pattern Recognition*, Las Vegas, NV, USA, 779–788. <https://doi.org/10.1109/CVPR.2016.91>
- Sanaeifar, A., Guindo, M.L., Bakhshipour, A., Fazayeli, H., Li, X., & Yang, C. (2023). Advancing precision agriculture: The potential of deep learning for cereal plant head detection. *Computers and Electronics in Agriculture*, **209**, 107875. <https://doi.org/10.1016/j.compag.2023.107875>
- Shen, Y., Zhou, H., Li, J., Jian, F., & Jayas, D.S. (2018). Detection of stored-grain insects using deep learning. *Computers and Electronics in Agriculture*, **145**, 319–325. <https://doi.org/10.1016/j.compag.2017.11.039>
- Singh, A., Jones, S., Ganapathysubramanian, B., Sarkar, S., Mueller, D., Sandhu, K., & Nagasubramanian, K. (2021). Challenges and opportunities in machine-augmented plant stress phenotyping. *Trends in Plant Science*, **26**(1), 53–69. <https://doi.org/10.1016/j.tplants.2020.07.010>
- Solahudin, M., & Mutawally, F.W. (2020). Identifikasi ganoderma pada tanaman kelapa sawit berbasis reflektansi gelombang multispektral. *Jurnal Keteknik Pertanian*, **7**(3), 193–200. <https://doi.org/10.19028/jtep.07.3.193-200>
- Solahudin, M., Pramudya, B., Liyantono, L., Supriyanto, S., & Manaf, R. (2015). Gemini virus attack analysis in field of chili (*Capsicum Annuum* L.) using aerial photography and bayesian segmentation method. *Procedia Environmental Sciences*, **24**, 254–257. <https://doi.org/10.1016/j.proenv.2015.03.033>
- Supyani, Poromarto, S.H., Supriyadi, Permatasari, F.I., Putri, D.H., Putri, D.T., & Hadiwiyono. (2021). Disease intensity of moler and yield losses of shallot cv. Bima caused by *Fusarium oxysporum f.sp. cepae* in Brebes Central Java. *IOP Conference Series: Earth and Environmental Science*, **905**, 012049. <https://doi.org/10.1088/1755-1315/905/1/012049>
- Susilawati, D.M., Maarif, M.S., Widiatmaka, & Lubis, I. (2019). Evaluasi kesesuaian dan ketersediaan lahan untuk pengembangan komoditas bawang merah di Kabupaten Brebes, Provinsi Jawa Tengah. *Jurnal Pengelolaan Sumberdaya Alam dan Lingkungan*, **9**(2), 507–526. <https://doi.org/10.29244/jpsl.9.2.507-526>
- Wang, C.Y., Bochkovskiy, A., & Liao, H.Y.M. (2023). YOLOv7: Trainable bag-of-freebies sets new state-of-the-art for real-time object detectors. *2023 IEEE/CVF Conference on Computer Vision and Pattern Recognition (CVPR)*, Vancouver, BC, Canada: 7464-7475. <https://doi.org/10.1109/CVPR52729.2023.00721>
- Yang, J., Duan, Y., Liu, X., Sun, M., Wang, Y., Liu, M., Zhu, Z., Shen, Z., Gao, W., Wang, B., Chang, C., & Li, R. (2022). Reduction of banana fusarium wilt associated with soil microbiome reconstruction through green manure intercropping. *Agriculture, Ecosystems and Environment*, **337**, 108065. <https://doi.org/10.1016/j.agee.2022.108065>
- Zhang, F., Ren, F., Li, J., & Zhang, X. (2022). Automatic stomata recognition and measurement based on improved YOLO deep learning model and entropy rate superpixel algorithm. *Ecological Informatics*, **68**, 101521. <https://doi.org/10.1016/j.ecoinf.2021.101521>